www.elsevier.nl/locate/jorganchem
Journal of Organometallic Chemistry 611 (2611) 12–19

Journal of Organo metallic Chemistry

Review

Synthesis and structures of polysilacage compounds containing a silicon–silicon inter-element linkage

Masaki Shimizu [a], Tamejiro Hiyama [a,*1], Toshiaki Matsubara [b,*2], Tokio Yamabe [b]

[a] *Department of Material Chemistry, Graduate School of Engineering, Kyoto University, Yoshida, Sakyo-ku, Kyoto 606-8501, Japan*
[b] *Institute for Fundamental Chemistry, 34-4, Takano-Nishihiraki-cho, Sakyo-ku, Kyoto 606-8103, Japan*

Received 4 March 2000; received in revised form 17 April 2000; accepted 18 April 2000

Abstract

To explore the possibility of three-dimensional σ-conjugation originated from silicon–silicon inter-element linkages, 2,2,3,3,5,5,6,6,7,7,8,8-dodecamethyl-2,3,5,6,7,8-hexasilabicyclo[2.2.2]octane (**1**) was synthesized as a model compound. The molecular structure of **1** was shown to be slightly distorted from an ideal bicyclo[2.2.2]octane skeleton by X-ray analysis. Functionalization of **1** at bridgehead positions was achieved by treatment with BuLi–*t*-BuOK followed by a reaction with an electrophile. UV spectra of **1** and its derivatives demonstrated a bathochromic shift, particularly when dimensions of the molecular structure increased and a silyl or stannyl group was introduced at the bridgehead. This fact was understood in terms of three-dimensional σ-conjugation between silicon–silicon linkages. Computational study of model structures is also described. © 2000 Elsevier Science S.A. All rights reserved.

Keywords: Silicon–silicon bonds; Cage compounds; Bicyclo[2.2.2]octanes; σ-conjugation; Theoretical calculations

1. Introduction

Since silicon–silicon σ-bonds have relatively high energy level comparable to carbon–carbon double bonds, σ-conjugation of silicon–silicon linkages is possible. Indeed, unique electro-optical properties of organopolysilanes are attributed to the σ-conjugation along the linear skeleton [1]. Furthermore, very recently, σ-electrons of linear heterocatenates containing an –Si–Si–C– or –Si–Si–Si–Si–C– linkage were found to be delocalized along the acyclic framework [2]. On the other hand, the extension of a linear π-conjugate system consisting of carbon–carbon double bonds, e.g. polyacetylenes, to a three-dimensional π-conjugate system like barrelene or C_{60} is attractive in view of exploration for new materials [3]. In analogy, a three-dimensional σ-conjugate system consisting of silicon–silicon σ-bonds might lead to the evolution of organic materials that perform electronic communication. Based on this idea, we designed 2,2,3,3,5,5,6,6,7,7,8,8-dodecamethyl - 2,3,5,6,7,8 - hexasilabicyclo[2.2.2]octane (**1**), in which three silicon–silicon linkages are aligned in parallel between two bridgehead carbons. We considered this compound would exemplify three-dimensional σ-conjugation (Fig. 1) [4]. In this article, we describe the synthesis and properties of **1** and its derivatives as well as theoretical calculations of their structures [5]. We also describe the synthesis of trisilane-containing cage compounds [6].

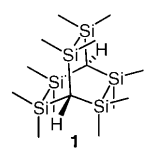

Fig. 1. 2,2,3,3,5,5,6,6,7,7,8,8-Dodecamethyl-2,3,5,6,7,8-hexasilabicyclo[2.2.2]octane.

[1] *Corresponding author. Tel./fax: +81-75-753-5555; e-mail: thiyama@npc05.kuic.kyoto-u.ac.jp.
[2] *Corresponding author.

PII: S0022-328X(00)00485-X

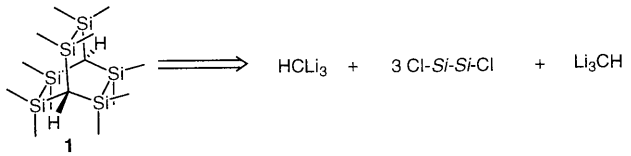

Scheme 1. Retrosynthesis of **1**.

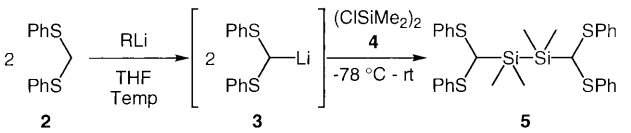

RLi	Temp (°C)	Yield (%)
t-BuLi	-42 - 0	35
s-BuLi	-30	77
n-BuLi	-30	82
n-BuLi	0	94

Scheme 2. Synthesis of **5** from **2**.

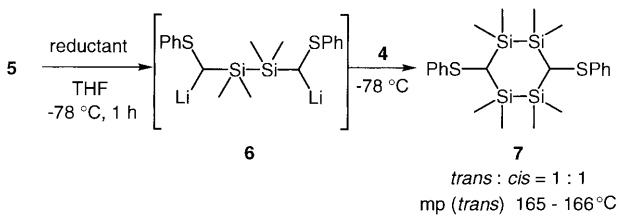

Reductant	Mol amounts	Yield (%)
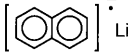	2.1 x 2	52
	2.5 x 2	57
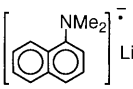	3.3 x 2	79
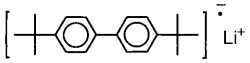	2.1 x 2	62
	2.5 x 2	65
(LDBB)	3.0 x 2	82

Scheme 3. Synthesis of **7** from **5**.

2. Synthesis of 1

Our synthetic approach toward **1** is conceptually based on triple silylation of two molecules of a trilithiomethane equivalent with three molecules of dichlorodisilane as illustrated in Scheme 1. For a trilithiomethane equivalent, we selected commercially available bis(phenylthio)methane (**2**), because the phenylthio group facilitates deprotonation and stabilizes the resulting anionic center. Moreover, the group is readily removed by metalation to give rise to the lithium reagent.

At first, we treated **2** with an alkyllithium under the conditions shown in Scheme 2 to generate bis(phenylthio)methyllithium (**3**) and silylated with 1,2-dichloro-1,1,2,2-tetramethyldisilane (**4**) at −78°C. Disilane **5** was best obtained in 94% yield when the deprotonation was effected with BuLi at 0°C.

Next, reduction of **5** with lithium radical anion and its silylation with **4** was effected as shown in Scheme 3. The most effective was the use of LDBB (6 mol) for **5** (1 mol), giving **7** in 82% yield as a stereoisomeric mixture (*cis*:*trans* = 1:1). The *trans* isomer could be isolated as a colorless solid (m.p. 165–166°C) by recrystallization of the stereoisomeric mixture from hexane.

Final ring formation for hexasilabicyclo[2.2.2]octane (**1**) was attained by reduction of **7** with LDBB and subsequent silylation with **4** (Scheme 4). Thus, to a 0.13 M THF solution of LDBB was added at −78°C a 1 M THF solution of **7** (a 1:1 mixture of stereoisomers). The resulting solution was stirred at −78°C for 15 min. A 0.05 M solution of **4** in THF was slowly added to the reaction mixture at −42°C to give **1** as colorless prisms (m.p. 283–284°C) in 73% yield along with 1,1,2,2,4,4,5,5-octamethyl-1,2,4,5-tetrasilacyclohexane (**9**) in 5% yield.

Single crystals of **1** suitable for X-ray measurement were obtained by recrystallization from cyclohexane. The ORTEP drawing of **1** is shown in Fig. 2. The molecule possesses one C_2 axis passing through the midpoints of the C(1)–C(1)* line and the Si(3)–Si(3)* bond. The molecular structure is slightly distorted from an ideal bicyclo[2.2.2]octane geometry and the lengths of three Si–Si bonds range from 2.369(1)–2.373(2) Å, slightly longer than 2.34 Å of a normal Si–Si bond, probably due to the steric repulsion between the methyl

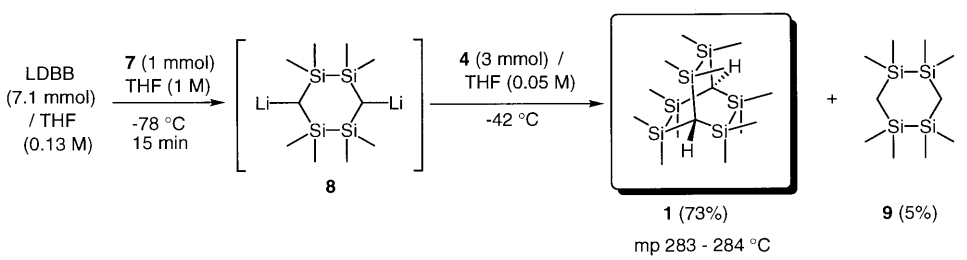

Scheme 4. Synthesis of **1** from **7**.

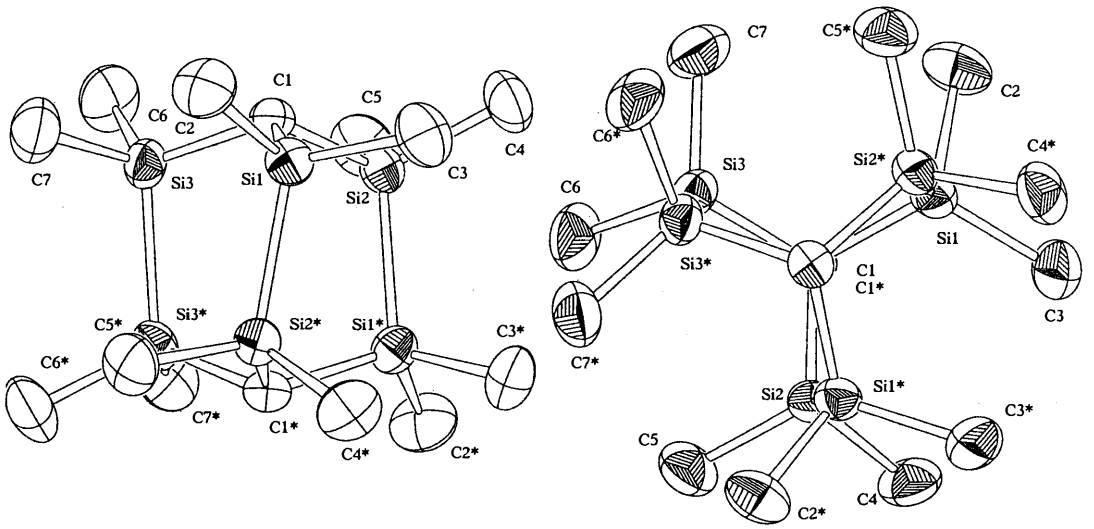

Fig. 2. Molecular structure of **1**.

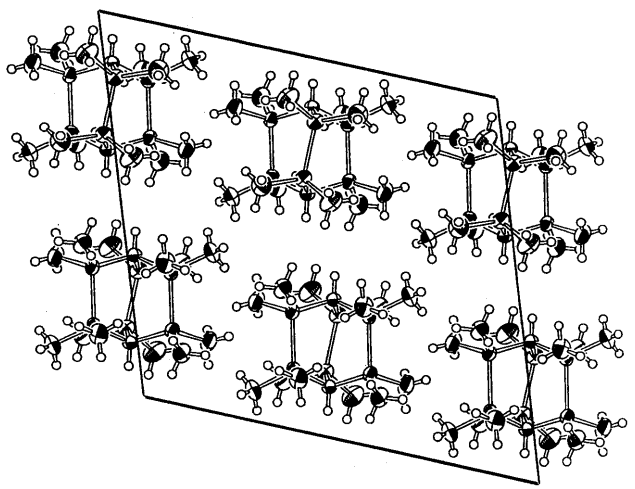

Fig. 3. Packing diagram of **1**.

groups oriented in a nearly eclipsed position. The angle deviation from the perfectly eclipsed arrangement of C(1)–Si(1) and C(1)*–Si(2)* bonds is about 12° which is also observed in other pairs of C(1)–Si or C(1)*–Si bonds. Furthermore, the packing diagram shown in Fig. 3 illustrates that the molecules form layers and Si–Si bonds are aligned parallel and almost perpendicular to each layer.

3. Derivatization of 1

To functionalize at bridgehead carbons, we screened various bases and found a superbase (> 2 mol) made from BuLi and *t*-BuOK was highly effective to generate a monolithio derivative of **1** and after silylation obtained **10a** in nearly quantitative yields (Scheme 5). It is noteworthy that only monosilylation occurred; bis-silylation never took place in spite of the presence of the base and Me_3SiCl in excess. Probably through-space or through-bond electrostatic interaction prevented the formation of a bridgehead dianion.

The stability of the bridgehead carbanion **11** was next examined. Anion **11** generated from **1** (1 mol) and the superbase (4 mol) at −42°C for 1 h was allowed to warm to the temperature specified in Scheme 6 and kept for 10 min before trimethylsilylation. To our surprise, anion **11** was found to be stable even at room temperature owing possibly to three anion-stabilizing silicon atoms.

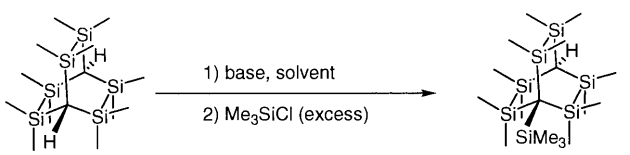

Base (mol)	Solvent	Temp (°C)	Yield (%)
MeLi (2.0)	THF-Et_2O	reflux	44 (NMR)
BuLi-*t*-BuOK (1.2)	THF	-42	70 (NMR)
BuLi-*t*-BuOK (2.0)	THF	-42	98
BuLi-*t*-BuOK (3.0)	THF	-42	96
BuLi-*t*-BuOK (6.0)	THF	-42	97

Scheme 5. Silylation of **1** at a bridgehead position.

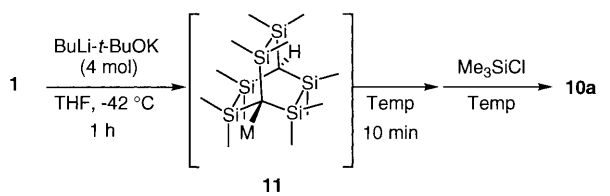

Temp (yield of **10a**) : -42 °C (96%); -20 °C (95%); rt (96%); 50 °C (82%)

Scheme 6. Anion stability of **11**.

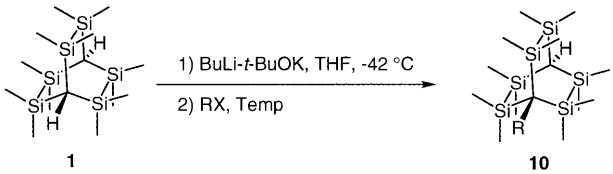

RX	Temp (°C)	10	R	Yield (%)
$Me_2PhSiCl$	-42	**10b**	$SiPhMe_2$	90
$Me_2[Cl(CH_2)_3]SiCl$	-42	**10c**	$SiMe_2[(CH_2)_3Cl]$	86
Bu_3SnCl	-42 to rt	**10d**	$SnBu_3$	88
MeI	-42	**10e**	Me	97
$CH_2{=}CHCH_2Br$	-42	**10f**	$CH_2CH{=}CH_2$	94
$PhCH_2Br$	-42 to rt	**10g**	CH_2Ph	85
$(PhS)_2$	-42 to rt	**10h**	SPh	62
I_2	-42	**10i**	I	77

Scheme 7. Functionalization of **1** at a bridgehead carbon.

In this way, various electrophiles were introduced at the bridgehead of **1**, giving rise to **10b**–**10i** in good to excellent yields (Scheme 7).

Although direct dimetalation at the bridgehead carbons in **1** was not successful, a stepwise procedure involving deprotonation of **10** followed by electrophilic quenching allowed us to prepare symmetrically or dissymmetrically disubstituted derivatives **13** or **14** (Scheme 8).

4. UV spectra of cage compounds

UV absorption spectra of **1**, **9**, **10a**, **10d**, **12**, and $(Me_3Si)_2$ measured in cyclohexane (0.1 mM) at room temperature are shown in Fig. 4: λ_{max} and ε of **9** (201 nm, $\varepsilon = 12\,500$), **1** (206 nm, $\varepsilon = 16\,400$), **10a** (209 nm, $\varepsilon = 19\,300$), **10d** (215 nm, $\varepsilon = 26\,200$; 233 nm, $\varepsilon = 13\,700$) and

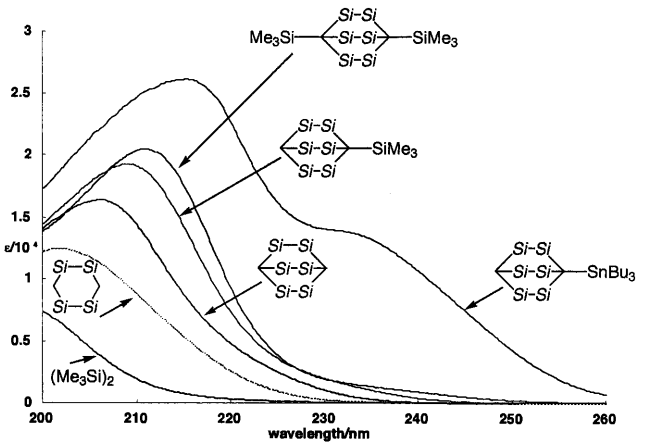

Fig. 4. UV spectra of $(Me_3Si)_2$, **1**, **9**, **10a**, **10c**, **12**.

12 (211 nm, $\varepsilon = 20\,500$) exhibit a bathochromic shift when the molecular dimension increases and more when a trimethylsilyl or tributylstannyl group is introduced at the bridgehead.

5. Theoretical calculation of the structures of cage compounds

We carried out ab initio MO calculations for $(SiH_3)_2$, **9′**, **1′**, **10a′**, **10d′**, **10e′**, and **12′**. Here all methyl or butyl substituents in $(SiMe_3)_2$, **9**, **1**, **10a**, **10d**, **10e**, and **12**, respectively, were replaced by hydrogen, and unless otherwise noted the dihedral angle ∠C–Si–Si–C in **1**, **10**, and **12** was fixed at 12° as experimentally observed in **1**. We at first optimized each geometry with basis set I consisting of 6-31G* for Si and C, 6-31G for H, and 3-21G* for Sn. On the basis of the optimized structures,

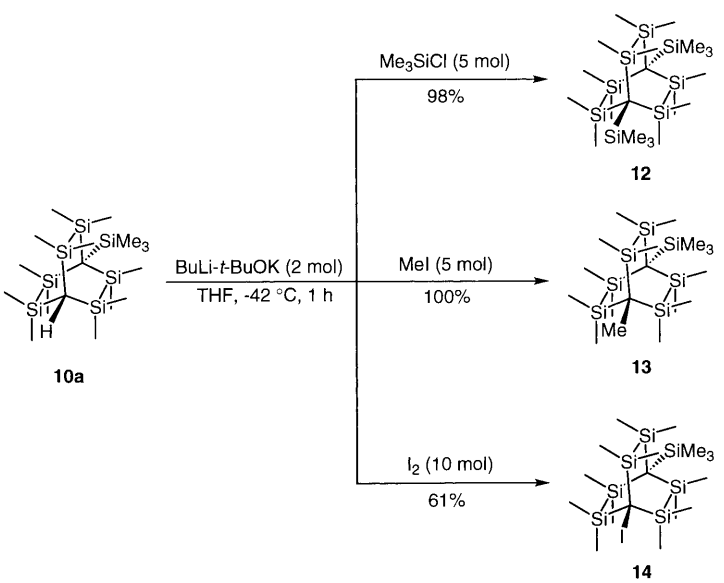

Scheme 8. Second functionalization of **10a**.

Table 1
Selected optimized parameters (Å and °) for $(SiH_3)_2$, **9′**, **10′**, and **12′** at B3LYP/I level

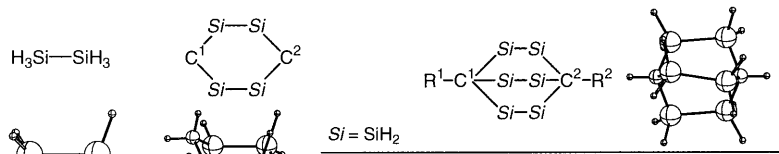

	$(SiH_3)_2$	**9'**	R^1 / R^2 H / H **1'**	CH_3 / H **10e'**	SiH_3 / H **10a'**	SiH_3 / SiH_3 **12'**	SnH_3 / H **10d'**
Si-Si	2.351	2.360	2.374	2.375	2.375	2.376	2.376
C^1-Si	–	1.902	1.904	1.910	1.908	1.906	1.898
C^2-Si	–	1.902	1.904	1.902	1.903	1.906	1.903
$\angle R^1$-C-Si	–	–	108.8	110.8	110.3	110.6	109.8
$\angle R^2$-C-Si	–	–	108.8	109.2	109.0	110.6	109.0
$\angle$Si-C^1-Si	–	114.0	110.1	108.1	108.6	108.4	109.1
$\angle$Si-C^2-Si	–	114.0	110.1	109.8	109.9	108.4	109.0
$\angle C^1$-Si-Si	–	110.5	107.6	109.9	109.3	109.3	108.9
$\angle C^2$-Si-Si	–	110.5	107.6	107.7	107.6	109.3	107.5

we calculated energies with the higher quality basis set II, where 6-31G* for Si and C is replaced by 6-31 + G*. Selected optimized parameters at B3LYP/I level are presented in Table 1.

Comparison of $(SiH_3)_2$, **9′**, **1′**, **10a′**, **10d′**, **10e′**, and **12′**, shows an Si–Si bond distance increase in the order, **1′**, **10′** and **12′** > **9′** > $(SiH_3)_2$; angles ∠Si–C–Si and ∠C–Si–Si are larger in **9′** than in **1′**, **10′** and **12′**. Introduction of CH_3, SiH_3, and SnH_3 at the bridgehead of **1′** increases angles ∠R–C–Si and ∠C–Si–Si and decreases the angle ∠Si–C–Si. Distortion effect on the geometry and energy was examined with dihedral angles ∠Si–C–C–Si of 0°, 6°, 12°, 18°, and 24°, and **1′** was found to be the most stable at a dihedral angle of 0° (Table 2).

The structure with dihedral angle ∠Si–C–C–Si of 12° was 1.3 kcal mol^{-1} higher in energy than that with 0°. When constraint on the dihedral angle was released, the dihedral angle was relaxed from 12° to 0°. This indicates that the distortion with dihedral angle of 12° observed experimentally by X-ray analysis comes from the steric repulsion between methyl substituents on silicon atoms. Selected geometrical parameters at various dihedral angles are also presented in Table 2, which indicates that some bond angles are influenced by the dihedral angle. Upon increasing the dihedral angle, angle ∠H–C–Si increases and angles ∠Si–C–Si and ∠C–Si–Si decrease, whereas the distances of Si–Si and C–Si bonds remain roughly constant.

Calculation at B3LYP/II level of the energy for the optimized structures of $(SiH_3)_2$, **9′**, **1′**, **10a′**, **10d′**, **10e′**, and **12′** with a dihedral angle of 12° gave energies of Si–Si σ and Si–Si σ* orbitals as presented in Table 3.

The Si–Si σ and Si–Si σ* orbitals of each compound located at HOMO and LUMO regions, respectively. The energy gap of Si–Si σ and Si–Si σ* orbitals decreases in the order $(SiH_3)_2$ > **9′** > **10e′** > **1′** > **10a′** > **12′** > **10d′**. The results are consistent with the

Table 2
Selected optimized parameters(Å and °) at B3LYP/I level and the calculated relative energies and the molecular orbital (MO) energies (ε) for Si–Si σ and Si–Si σ* orbitals and the energy gap between them (Δε) at B3LYP/II level for **1′** with the various ∠Si–C–C–Si bond angles

∠Si–C–C–Si	**0**	**6**	**12**	**18**	**24**
Si–Si	2.375	2.375	2.374	2.376	2.383
C–Si	1.904	1.904	1.904	1.905	1.906
∠H–C–Si	108.2	108.4	108.8	109.5	110.2
∠Si–C–Si	110.7	110.5	110.1	109.5	108.7
∠C–Si–Si	108.2	108.1	107.6	106.8	105.5
Relative energy (kJ mol^{-1})	0	0.2	1.3	5.9	16.7
MO energy ε (a.u.)					
Si–Si σ*	−0.00037	−0.00035	−0.01891	−0.01501	−0.01347
Si–Si σ	−0.27749	−0.27739	−0.27689	−0.27607	−0.27454
Δε (kJ mol^{-1})	727.6	727.2	677.4	685.3	685.3

Table 3
The calculated molecular orbital (MO) energies (ε) for Si–Si σ and Si–Si σ* orbitals and the energy gap between them ($\Delta\varepsilon$) for $(SiH_3)_2$, **9′**, **10**, and **12** at B3LYP/II level, and the UV absorption experimentally observed for the corresponding compounds

	$Si(H_3)_2$	**9′**	**1′**	**10e′**	**10a′**	**12′**	**10d′**
MO energy ε (a.u.)							
Si–Si σ*	−0.00363	−0.01155	−0.01891	−0.01842	−0.02285	−0.02668	−0.02318
Si–Si σ	−0.30211	−0.27551	−0.27689	−0.28059	−0.26995	−0.26532	−0.25767
$\Delta\varepsilon$ (kJ mol^{-1})	782.9	692.9	677.4	688.3	648.9	626.3	615.7
Experimental							
λ_{max} (nm)	>200	201	206	206	209	211	215
ν ($\times 10^4$ cm^{-1})		4.98	4.85	4.85	4.78	4.74	4.65

bathochromic shift observed with the methylated compounds. We found that the decrease in energy gap is caused by the stabilization of Si–Si σ orbitals and destabilization of Si–Si σ* orbitals. In order to clarify the influence of the distortion in **1**, we examined the change in the energy gap between the Si–Si σ and Si–Si σ* orbitals, changing the dihedral angle ∠Si–C–C–Si from 0° to 24°. As is presented in Table 2, the energy gap decreased with increase of the dihedral angle from 0° to 12°, whereas no explicit change was found above 12°.

The unique electronic and optical phenomena in organopolysilanes, such as bathochromic shifts, are very often interpreted in terms of σ conjugation. It has been reported that the stability in energy of both Si–Si σ and Si–Si σ* orbitals that lie on the HOMO–LUMO region is strongly influenced by σ conjugation, which destabilizes Si–Si σ orbitals and stabilizes Si–Si σ* orbitals to reduce the energy gap between the Si–Si σ and Si–Si σ* orbitals. In models **9′**, **1′**, **10a′**, **10d′**, **10e′**, and **12′** having a high dimensional structure, for example, the HOMO orbital, in which the pσ orbitals of bridgehead carbon as well as Si–Si σ orbitals contribute, can form a cyclic σ conjugated system as shown in Fig. 5.

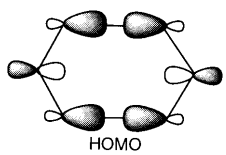

Fig. 5. An illustration of molecular orbital of HOMO.

In **1′**, **10′**, and **12′** which have small ∠Si–C–Si and ∠C–Si–Si angles compared with **9′**, the cyclic σ conjugation would be enhanced, because the pσ orbitals of bridgehead carbon and Si–Si σ orbitals are aligned close to each other.

The HOMOs of **1′**, **10a′**, **10d′**, and **10e′** are presented in Fig. 6. Remarkable differences among **1′**, **10a′**, **10d′**,

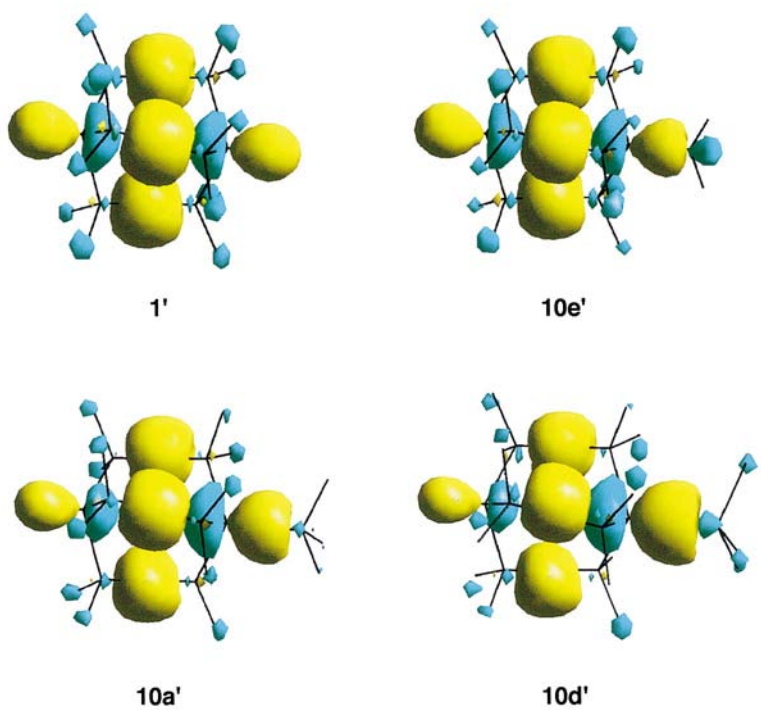

Fig. 6. Three-dimensional molecular orbital of HOMO for **1′**, **10e′**, **10a′**, and **10d′**.

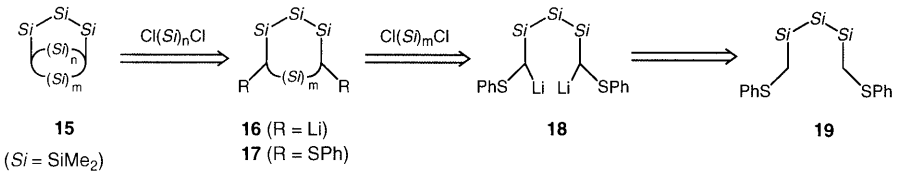

Scheme 9. Retrosynthesis of **15**.

and **10e′** are the degree of expansion of pσ orbital lobes directing to the inside of the cage molecules. The expansion of the pσ orbital lobe is larger in the order **10d′** > **10a′** > **10e′** ≈ **1′**, due to the electronic effect of a substituent at the bridgehead carbon. Since large inward expansion of the pσ orbital apparently induces more σ conjugation and reduces the energy gap between the Si–Si σ and Si–Si σ* orbitals, the experimentally observed bathochromic shift among **1′**, **10a′**, **10d′**, and **10e′** is reasonably understood.

6. Synthesis and UV properties of cage compounds containing a trisilane linkage

The above observations disclosed the possibility of three-dimensional σ-conjugation in cage molecules with a disilane bridge. To gain more information on the σ-conjugation in polysilacage compounds, we designed the cage molecule **15** that has a trisilane bridge. We selected 1,5-bis(phenylthio)-1,5-dilithio-2,3,4-trisilapentane (**18**) as a dimetallic reagent containing a trisilane unit, wherein a phenylthio group could facilitate its generation, stabilize the anionic carbons, and be easily reduced by lithium radical anions to afford requisite dianionic reagent **16** via initial polysilacycloalkanes **17** (Scheme 9).

At the outset, **19** was treated successively with LDBB in THF at low temperatures and then with dichlorodimethylsilane to give 1,2,3,5-tetrasilacyclohexane (**20a**) as a stereoisomeric mixture (*cis*:*trans* = 1:1) (Table 4, runs 1–3) in moderate yields. The successful ring formation is of synthetic value in view of the steric bulk of the octamethyltetrasilacyclohexane ring. Reductive lithiation of **19** and silylation with **4** at −78°C gave pentasilacycloheptane (**20b**) in 69% yield (run 4), whereas no cyclization occurred with 1,3-dichloro-1,1,2,2,3,3-hexamethyltrisilane (run 5) due probably to steric hindrance.

Table 4
Synthesis of **20** via reductive lithiation of **19**

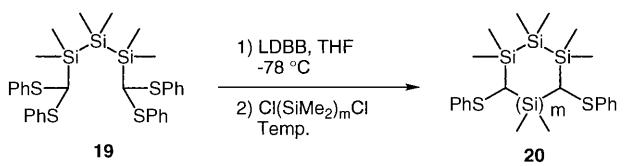

Run	m	Temp (°C)	**20**	Yield%
1	1	−98	**20a**	47
2	1	−78	**20a**	50
3	1	−30	**20a**	27
4	2	−78	**20b**	69
5	3	−78	**20c**	0

Since purification of **20** was tedious due to contaminants like benzenethiol, **16** was also generated by deprotonation of **21** with a base as shown in Eq. (1). The most effective was the use of *s*-BuLi at −30°C, giving **20a** in 51% yield, comparable to the reductive lithiation protocol.

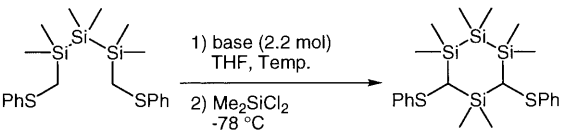

(1)

s-BuLi, -50 °C (38%); *s*-BuLi, -30 °C (51%); BuLi/*t*-BuOK, -78 °C (32%)

With **20a** in hand, we next studied the generation of a cyclic dianion reagent and its cyclization toward the cage compounds (Scheme 10). Reduction of **20a** (1:1 stereoisomeric mixture) with LDBB effectively produced cyclic 1,3-dimetallic reagent **16** ($m = 1$) which, upon quenching with aq. NH_4Cl, gave 1,2,3,5-tetrasilacyclohexane (**22**) in 82% yield. Silylation of **16** ($m = 1$) with dichlorodimethylsilane or **4** at −40°C proceeded successfully, giving rise to 2,3,4,6,7-pentasilabicyclo[3.1.1]heptane (**23**) or 2,3,4,6,7,8-hexasilabicyclo[3.2.1]octane (**24**) in 62% or 63% yield, respectively. Since the yields more than 50% mean that both stereoisomers of **20a** were converted into the cyclic products, epimerization appears to have occurred at −40°C during metalation or silylation.

UV absorption spectra of octamethyltrisilanes, **22**, **23**, and **24** measured in cyclohexane (1×10^{-4} M) at room temperature are shown in Fig. 7. λ_{max} of octamethyltrisilane (217 nm, $\varepsilon = 7590$), **22** (223 nm, $\varepsilon = 6130$), **23** (225 nm, $\varepsilon = 5720$), and **24** (223 nm, $\varepsilon = 7780$) clearly exhibit a bathochromic shift on going from acyclic to cyclic and further to bicyclic structures.

7. Summary

We have disclosed a novel strategy for the synthesis of hexasilabicyclo[2.2.2]octanes (**1**, **10**, and **12**–**14**) and trisilane-containing cage compounds (**23** and **24**). On the basis of UV spectra and calculations, three-dimensional

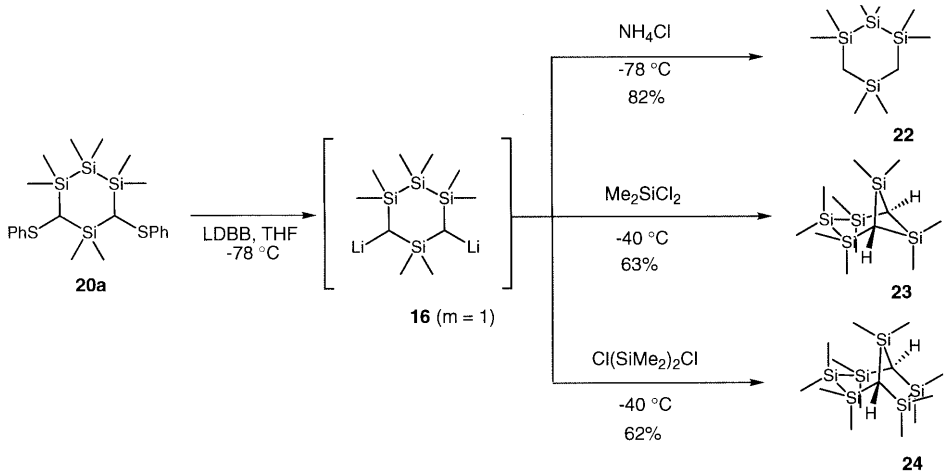

Scheme 10. Synthesis of trisilane linkage-containing silanes **22**–**24**.

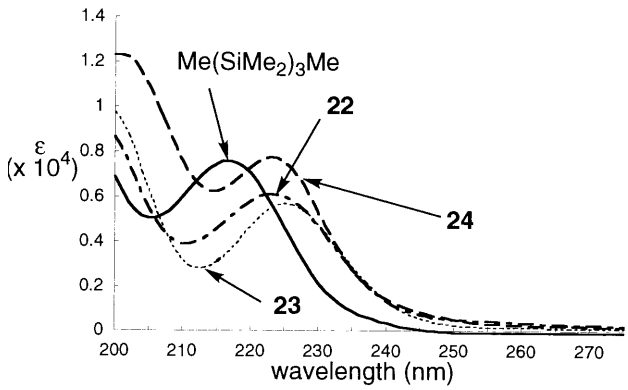

Fig. 7. UV spectra of octamethyltrisilane, **22**, **23**, and **24**.

σ-conjugation is concluded to exist in such polysilacage compounds. Further extension of the synthetic strategy and applications to organic materials are in progress.

Acknowledgements

This work was supported by a Grant-in-Aid for Scientific Research on Priority Areas, The Chemistry of Inter-element Linkage (No. 09239102) from the Ministry of Education, Science, Sports and Culture, Japan and a Grant-in-Aid for Research for the Future Program (96R11601) from The Japan Society of the Promotion of Science. M.S. acknowledges financial support from the Nissan Science Foundation and Arakawa Chemical Industries, Ltd. We are grateful to Professor Atsunori Mori in the Tokyo Institute of Technology for valuable discussions, to Dr Yasushi Nishihara in the Tokyo Institute of Technology, Professor Koji Tanaka, and Dr Kiyoshi Tsuge in the Institute for Molecular Science for X-ray diffraction analysis, and to Dr Kiyoshi Fujisawa in the Tokyo Institute of Technology for UV-spectra measurement. We also thank Shin-Etsu Chemical Co. Ltd. for generous gifts of organosilicon reagents.

References

[1] Reviews of organopolysilanes: (a) M. Kumada, K. Tamao, Adv. Organomet. Chem. 6 (1968) 19. (b) H. Sakurai, J. Organomet. Chem. 200 (1980) 261. (c) R. West, in: G. Wilkinson, F.G.A. Stone, E.W. Abel (Eds.), Comprehensive Organometallic Chemistry, vol. 2, Pergamon, Oxford, 1982, pp. 365–397. (d) R. West, J. Organomet. Chem. 300 (1986) 327. (e) R.D. Miller, J. Michl, Chem. Rev. 89 (1989) 1359. (f) R. West, in: E.W. Abel, F.G.A. Stone, G. Wilkinson (Eds.), Comprehensive Organometallic Chemistry II, vol. 2 Pergamon, Oxford, 1995, pp. 77–110. Reviews of cyclic and cage organopolysilanes: (g) E.F. Hengge, J. Organomet. Chem. Lib. 9 (1979) 261. (h) R. West, Pure Appl. Chem. 54 (1982) 1041. (i) H. Watanabe, Y. Nagai, in: H. Sakurai (Ed.), Organosilicon and Bioorganosilicon Chemistry: Structure, Bonding, Reactivity and Synthetic Application, Ellis Horwood, Chichester, 1985, pp. 107–114. (j) T. Tsumuraya, S.A. Batcheller, S. Masamune, Angew. Chem. Int. Ed. Engl. 30 (1991) 902. (k) A. Sekiguchi, H. Sakurai, Adv. Organomet. Chem. 37 (1995) 1.

[2] (a) H. Isaka, H. Teramae, M. Fujiki, N. Matsumoto, Macromolecules 28 (1995) 4733. (b) T. Sanji, H. Hanao, H. Sakurai, Chem. Lett. (1997) 1121.

[3] (a) W.E. Billups, M.A. Ciufolini (Eds), Buckminsterfullerenes, VCH, New York, 1993. (b) K. Prassides (Ed.), Physics and Chemistry of the Fullerenes, NATO ASI Series C, Kluwer Academic Publishers, Dordrecht, 1994.

[4] Tetradecamethylbicyclo[2.2.2]octasilane whose skeleton was made up entirely of silicon was reportedly prepared in 3–5% yields by Na/K or Li condensation of trichloromethylsilane and dichlorodimethylsilane. (a) R. West, A. Indriksons, J. Am. Chem. Soc. 94 (1972) 6110. (b) M. Ishikawa, M. Watanabe, J. Iyoda, H. Ikeda, M. Kumada, Organometallics 1 (1982) 317. Cage compounds $E(Me_2SiSiMe_2)_3E$ (E = P, As, Sb, Bi) were also synthesized to examine through-bond interactions of heteroatoms. (c) K. Hassler, J. Organomet. Chem. 246 (1983) C31. (d) K. Hassler, S. Seidl, J. Organomet. Chem. 347 (1988) 27. (e) U. Winkler, M. Schieck, H. Pritzkow, M. Driess, I. Hyla-Kryspin, H. Lange, R. Gleiter, Chem. Eur. J. 3 (1997) 874.

[5] M. Shimizu, N. Inamasu, Y. Nishihara, T. Hiyama, Chem. Lett. (1998) 1145.

[6] M. Shimizu, S. Ishizaki, H. Nakagawa, T. Hiyama, Synlett (1999) 1772.